EUKARYOTIC CELL, July 2008, p. 1136–1145 Vol. 7, No. 7
1535-9778/08/$08.00+0 doi:10.1128/EC.00102-08
Copyright © 2008, American Society for Microbiology. All Rights Reserved.

Partially Functional Outer-Arm Dynein in a Novel *Chlamydomonas* Mutant Expressing a Truncated γ Heavy Chain[▽]

Zhongmei Liu,[1]† Hiroko Takazaki,[2]† Yuki Nakazawa,[1] Miho Sakato,[3] Toshiki Yagi,[1,4] Takuo Yasunaga,[2] Stephen M. King,[3] and Ritsu Kamiya[1,5]*

Department of Biological Sciences, Graduate School of Science, University of Tokyo, Hongo, Bunkyo-ku, Tokyo[1]; Department of Bioscience and Bioinformatics, Kyushu Institute of Technology, Iizuka, Japan[2]; Department of Molecular, Microbial and Structural Biology, University of Connecticut Health Center, Farmington, Connecticut[3]; Structural Biology, Graduate School of Science, Kyoto University, Kyoto[4]; and CREST, Japan Science and Technology Corporation, Kawaguchi, Japan[5]

Received 21 March 2008/Accepted 6 May 2008

The outer dynein arm of *Chlamydomonas* flagella contains three heavy chains (α, β, and γ), each of which exhibits motor activity. How they assemble and cooperate is of considerable interest. Here we report the isolation of a novel mutant, *oda2-t*, whose γ heavy chain is truncated at about 30% of the sequence. While the previously isolated γ chain mutant *oda2* lacks the entire outer arm, *oda2-t* retains outer arms that contain α and β heavy chains, suggesting that the N-terminal sequence (corresponding to the tail region) is necessary and sufficient for stable outer-arm assembly. Thin-section electron microscopy and image analysis localize the γ heavy chain to a basal region of the outer-arm image in the axonemal cross section. The motility of *oda2-t* is lower than that of the wild type and *oda11* (lacking the α heavy chain) but higher than that of *oda2* and *oda4-s7* (lacking the motor domain of the β heavy chain). Thus, the outer-arm dynein lacking the γ heavy-chain motor domain is partially functional. The availability of mutants lacking individual heavy chains should greatly facilitate studies on the structure and function of the outer-arm dynein.

Dyneins are molecular motors that drive various kinds of microtubule-based motility, including intracellular vesicle transport and ciliary/flagellar beating. Axonemal dyneins, the motors responsible for ciliary and flagellar beating, are present as multiple species, which are generally classified into outer-arm and inner-arm dyneins according to their positions in the axoneme. The outer-arm dynein consists of a single species of a multisubunit complex containing two or three distinct dynein heavy chains (DHCs), each of which exhibits motor activity. The inner-arm dynein, in contrast, comprises multiple species, consisting of a two-headed dynein containing two different DHCs and multiple single-headed species, each containing a single DHC. Motility analyses of *Chlamydomonas* mutants lacking particular dynein species, and in vitro motility assays using isolated dyneins, have shown that the various dyneins differ in their motile properties, suggesting that regular axonemal beating is based on the coordinated function of multiple dynein motors with distinct properties (for reviews, see references 23 and 25). However, the mechanisms by which dynein motor function is coordinated within the axoneme are not understood.

How different DHCs coordinate with each other is an important issue also for the functioning of multiheaded dyneins such as the outer-arm dynein. This is because different outer-arm DHCs have been shown to display strikingly different in vitro motility in sea urchins (31, 45) and *Chlamydomonas* (41). The *Chlamydomonas* outer-arm dynein is composed of three DHCs (α, β, and γ), two intermediate chains (IC1 and IC2), and 11 light chains (LCs) (6, 25). The N-terminal third of each ~500-kDa DHC polypeptide is termed the tail or the stem, to which the two intermediate chains and most of the LCs are bound. The proximal region of the tail is the site where the three DHCs are associated with each other and attach to the A tubule of the outer doublet microtubule. The C-terminal region of each DHC consists of a AAA^+ ring structure with four phosphate-binding motifs (P-loops) and a microtubule-binding stalk; the general organization of this region is conserved in all dynein species. LC1 is associated with this domain of the γ DHC (2, 43). When isolated and adsorbed to a surface, the outer arm takes on a bouquet structure, with the three AAA^+ head domains projecting from the common base (11, 18, 47, 52). In the axoneme, this assembly is folded into a compact structure, which has been extensively studied using various electron microscopic techniques (10, 11, 17, 33, 34).

For studies aimed at elucidating the function and organization of individual DHCs in multiheaded dyneins, mutants missing a specific DHC are invaluable. In *Chlamydomonas*, mutants are available that lack the total outer arm (14, 21, 24, 29), only the α DHC (39), or the motor domain of the β DHC (40). The mutant lacking the α DHC, *oda11*, swims slower than the wild type but faster than mutants missing the entire outer arm, such as *oda2* and *oda4*. Thus, the outer-arm dynein containing only the β and γ DHCs can function in the axoneme, and the α DHC apparently increases the activity of the β/γ DHCs. The *oda4-s7* mutant, expressing only the N-terminal 160-kDa region of the β DHC and lacking its motor domain, assembles outer arms with the α and γ heavy chains, whereas the *oda4* mutant, with more severe defects in the β *DHC* gene, lacks the

* Corresponding author. Mailing address: Department of Biological Sciences, Graduate School of Science, University of Tokyo, 7-3-1 Hongo, Bunkyo-ku, Tokyo 113-0033, Japan. Phone: 81-3-5841-4426. Fax: 81-3-5841-4632. E-mail: kamiyar@biol.s.u-tokyo.ac.jp.
† These authors equally contributed to this study.
▽ Published ahead of print on 16 May 2008.

entire outer arm. In contrast to *oda11*, *oda4-s7* swims at almost the same speed as *oda4*. Thus, the motor domain of the β DHC appears to be essential for the function of the outer-arm dynein, and outer-arm dyneins containing only the α and γ DHCs are almost completely nonfunctional. However, it is not known how significantly the motor domain of the γ DHC contributes to overall outer-arm function.

The *oda11* and *oda4-s7* mutants were also useful for assigning the location of the α and β DHCs within the outer arm. Averaged outer-arm images in cross-section micrographs of the mutant axonemes located the α DHC at the tip of the outer arm and the motor domain of the β chain at an intermediate position between the base and tip (39, 40). From the combined images and the images of the *oda11 oda4-s7* double mutant, the γ DHC motor domain was predicted to localize to the inner lobe of the outer-arm image (40). These data have provided a basis for interpreting three-dimensional images obtained by cryo-electron microscopy and tomography (17, 33, 34).

Although *oda11* and *oda4-s7*, as well as other *oda* mutants lacking the entire arm, have greatly facilitated studies on the structure and function of outer-arm dyneins, another type of mutant has been awaited that lacks only the γ DHC motor domain. Such a mutant would greatly advance studies on the structure and function of individual DHCs. Here we report the isolation and characterization of such a mutant, *oda2-t*, which lacks only the motor domain of the γ DHC.

MATERIALS AND METHODS

Strains. The following *Chlamydomonas reinhardtii* strains were used: 137C (wild type), A54-e18 (a *nit1*$^-$ strain used for insertional mutagenesis; 46); the *oda2* strain lacking the entire outer dynein arm due to a mutation in the γ *DHC* gene (21); the *oda11* strain lacking the α DHC and the 16-kDa LC (LC5) of the outer arm due to a mutation in the α *DHC* gene (39); the *oda4-s7* strain lacking the motor domain of the outer-arm β DHC (40); the *pf14* strain lacking the radial spokes (12); and the *pf18* strain lacking the central pair (12).

Mutant isolation. A54-e18 was mutagenized by insertional mutagenesis (48) using a linearized plasmid DNA, pMN56, composed of the pUC119 vector sequence and the *NIT1* gene. Colonies were cultured on 96-well plates containing SGII/NO3 medium (12) and observed with an inverted microscope. Slow-swimming cells were examined for the composition of flagellar DHCs by urea sodium dodecyl sulfate-polyacrylamide gel electrophoresis (SDS-PAGE). Cells showing abnormal SDS-PAGE patterns were saved and mated with the wild type. Progenies of both mating types were saved.

Southern blot analysis. DNA was isolated from the *oda2-t* mutant and the parent (A54-e18) cells using the method of Weeks et al. (50). The DNA was digested with restriction enzymes, loaded on a 0.8% agarose gel, transferred to a Biodyne B membrane (PALL Life Science, Ann Arbor, MI), and hybridized with a 577-base-pair probe for the γ DHC gene. The probe was labeled with ^{32}P using a DNA labeling kit (Nippon Gene, Tokyo).

Immunoblotting assay. Axonemal polypeptides separated by SDS-PAGE in 5% or 10% acrylamide gels were transferred to a polyvinylidene difluoride membrane and incubated with monoclonal antibodies against γ DHC (12γB and 25-8) (27), LC2 (R5391) (35), and LC4 (CT61) (44). Antibody reactivity was visualized by color development with 5-bromo-4-chloro-3-indolyl phosphate and nitro blue tetrazolium (KPL, Gaithersburg, MD).

3′ RACE. For 3′ rapid amplification of cDNA ends (3′ RACE) (7), total RNA was isolated with TRIzol reagent (Invitrogen). Five micrograms of total RNA was subjected to reverse transcription using Superscript III reverse transcriptase (Invitrogen) and the specific adapter primer (5′-GGCCACGCGTCGACTAGT ACT_{17}.3′). The first-strand cDNA amplification was carried out with an Expand High Fidelity PCR system (Roche) and two primers, a gene-specific primer (5′-GGACGACCTGAAGCTCGACAACTAC-3′) and an abridged universal amplification primer (5′-GGCCACGCGTCGACTAGTAC-3′) (3′ RACE system; Invitrogen). Dimethyl sulfoxide was added to the reaction mixtures at a final concentration of 10%. Subsequent double-strand cDNA amplifications were carried out with five primers, designed based on the cDNA sequences of the γ DHC (http://www.ncbi.nlm.nih.gov; U15303) and NIT1 (AF203033).

DNA sequencing. The PCR product, or DNA extracted from gel slices, was purified using the Wizard SV gel and PCR clean-up system (Promega). DNA fragments were sequenced using the BigDye Terminator v3.1/1.1 cycle sequencing kit (Applied Biosystems).

Isolation of axonemes and fractionation of dynein. The culture of cells, isolation of flagella, preparation of crude dynein extract, and fractionation of dynein by high-pressure liquid chromatography on an ion-exchange column were as described by Kagami and Kamiya (20). Instead of a Mono Q column as previously used, a Uno Q column (Bio-Rad) was used, as it provides better separation of the outer-arm dyneins.

Electrophoresis. The composition of the flagellar DHCs was analyzed by urea SDS-PAGE with a 3 to 5% polyacrylamide gradient and a 3 to 8 M urea gradient (20). Intermediate chains and LCs were analyzed using SDS-PAGE with a 5 to 20% acrylamide gradient. All gels were stained with silver (4).

ATPase assay. The ATPase activities in the axonemes and extracts were assayed using EnzChek phosphate assay kit (Molecular Probes) in the presence of 1 mM ATP in HMDEK (30 mM HEPES [pH 7.4], 5 mM $MgSO_4$, 1 mM dithiothreitol, 1 mM EGTA, and 50 mM K-acetate) at 25°C. Under these conditions, the axonemes continued beating for >10 min. When the activity in the high-salt axonemal extract was measured, the sample also contained 60 mM KCl in addition to ATP and HMDEK. The absorbance at 360 nm was monitored for 5 min, and ATPase activity was determined from the rate of phosphate release. The measurements were performed in duplicate and repeated at least three times using different preparations for each sample.

Motility assessments. The swimming velocities of the mutant and wild-type cells were measured using a dark field microscope at a total magnification of ×100, a video recording system, and a personal computer. A red filter with a cutoff wavelength of 630 nm was used to suppress the response of the cells to light. The flagellar beat frequency was measured by analyzing the vibration of the cell bodies with a fast Fourier transform analyzer (22), which yields an approximate average of the beat frequencies in a large population of cells. All measurements were carried out in the Tris-acetate-phosphate medium at 25°C.

Motility of isolated axonemes was examined using the method of Bessen et al. (3). Movements were observed using a BX50 microscope (Olympus, Tokyo) equipped with a dark field condenser, a 40× objective (numerical aperture, 0.85), and a 100-W mercury arc lamp. The images were recorded with a high-speed charge-coupled-device video camera (HAS-200R; Ditect Co., Tokyo, Japan) operating at 200 frames/s.

Electron microscopy and image analysis. The axoneme samples were fixed with 2% glutaraldehyde in the presence of 2% tannic acid, postfixed with 1% OsO_4, dehydrated through a series of ethanol solutions, and embedded in Epon 812. Gray/silver sections, 60 to 80 nm thick, were cut, double-stained with uranyl acetate and lead citrate, and observed with a JEM1010 microscope (Jeol, Tokyo, Japan) at a magnification of ×40,000.

Image analysis was carried out basically following the protocol in reference 54 with some modifications. The cross sections of axonemes in which each doublet could be clearly seen as an assembly of protofilaments were selected. After the electron micrographs were corrected for the phase contrast transfer function following the estimated defocusing values, a set of images consisting of an outer doublet, inner and outer dynein arms, and the adjacent B tubule were boxed out as regions of interest (ROIs). All the ROIs were aligned so that they corresponded to the views seen from the proximal end of the axoneme. The ROIs were then classified by a hierarchical cluster analysis (55). The number of images used was 126 (wild type), 234 (*oda11*), 324 (*oda4-s7*), and 153 (*oda2-t*). In the analysis, a threshold was set so that the largest cluster in each sample contained more than 20 images. This resulted in classification into 7 (wild type), 12 (*oda11*), 19 (*oda4-s7*), and 9 (*oda2-t*) clusters. Each major cluster was refined, averaged, and normalized so that the difference between each mutant and the wild type could be detected by the Student *t* test.

RESULTS

A novel type of γ DHC mutant retaining the α and β DHCs. In an attempt to isolate new types of mutants deficient in flagellar function, we generated ~5,000 clones of *nit1*$^+$ transformants from a *nit1*$^-$ strain (A54-e18) and examined their motility phenotypes. Seven clones displayed jerky swimming, characteristic of *oda* mutants lacking outer-arm dyneins. SDS-PAGE of isolated axonemes indicated that six of them lacked

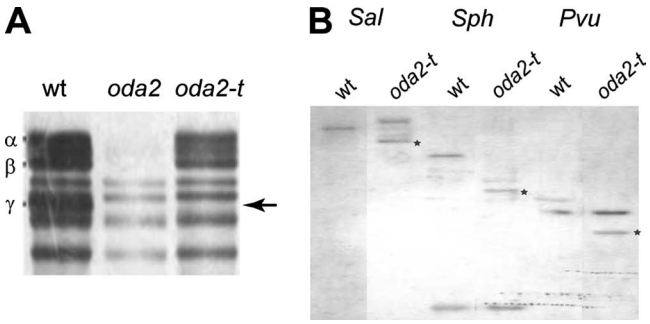

FIG. 1. The *oda2-t* mutant is defective in the γ DHC. (A) Part of a 3 to 5% urea SDS-PAGE pattern showing the DHC bands in the wild type (wt), *oda2*, and *oda2-t* axonemes. Wild-type axonemes have three outer-arm DHCs (α, β, and γ), which are completely absent in the *oda2* axonemes. The axonemes of *oda2-t* retain the α and β DHCs but lack the γ DHC (arrow). (B) Southern hybridization analysis of the γ *DHC* genes in A54-e18 (wt; control) and *oda2-t* genomic DNA digested with the restriction enzymes SalI, SphI, and PvuII and probed with a 577-base-pair fragment of the γ *DHC* gene (Fig. 3A). The stars indicate the bands that differ between A54-e18 and *oda2-t*.

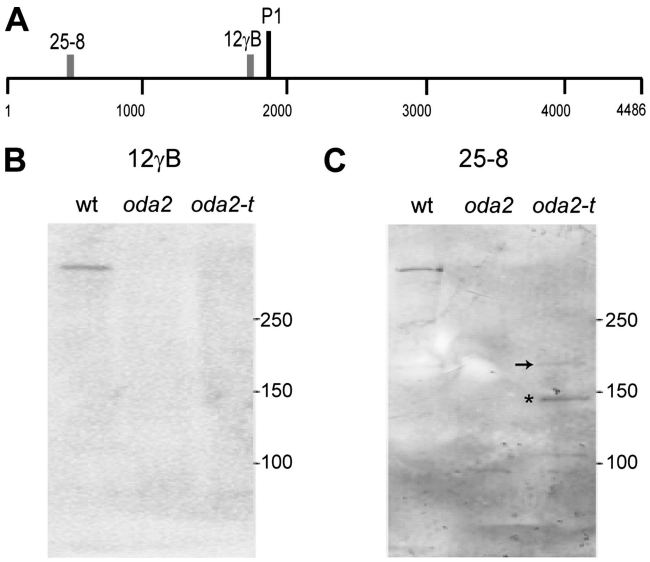

FIG. 2. *oda2-t* axonemes contain a truncated γ DHC. (A) Map of the γ DHC showing the P1 site in the motor domain and the regions recognized by monoclonal antibodies 12γB and 25-8, based on data from King and Witman (27) and Wilkerson et al. (51). (B and C) Immunoblot analyses of the wild type (wt), *oda2*, and *oda2-t* flagellar axonemes with antibodies 12γB (B) and 25-8 (C). As shown in panel B, the antibody 12γB detected the γ DHC band in the wild type but no bands in *oda2* or *oda2-t.* As shown in panel C, in contrast, the 25-8 antibody detected a DHC band in the wild type, nothing in *oda2*, and an ~180-kDa band (arrow), an ~150-kDa band (asterisk), and an ~105-kDa band in *oda2-t*.

the three outer-arm DHCs (α, β, and γ) (not shown), while one clone appeared to lack only the γ DHC, retaining the α and β DHCs (Fig. 1A). A genetic cross with *oda2*, a mutant lacking the entire outer-arm dynein due to a mutation in the γ *DHC* gene, did not yield wild-type daughter cells in 50 tetrads, suggesting that this clone is an *oda2* allele. To confirm that this mutant in fact has a mutation in the γ *DHC* gene, we carried out genomic Southern analysis using a specific probe for the γ *DHC* gene (Fig. 3A). The hybridization pattern in the DNAs from the parent and this mutant, after digestion with three restriction enzymes, differed (Fig. 1B). Thus, this clone most likely carries a mutation in the γ *DHC* gene. To distinguish this mutant from the previous *oda2* alleles lacking the entire outer arm, we named it *oda2-t*, because it produces a truncated γ DHC, as shown below.

Western blot analysis. Since the *oda2-t* mutant retains the α and β DHCs in the axoneme while the previously isolated *oda2* alleles lack the entire outer arm, we speculated that *oda2-t* expresses the N-terminal tail portion of the heavy chain. The necessity and sufficiency of the tail portion of DHCs for the assembly of dynein complexes in the axoneme have been shown for the outer-arm β DHC (40) and the inner-arm DHC10 (36). To confirm this for *oda2-t*, we carried out Western blot analyses using two γ DHC-specific monoclonal antibodies, 25-8 and 12γB. The epitope recognized by antibody 25-8 is located within approximately 43 kDa of the N terminus, whereas the 12γB epitope (Q1735 to Q1758) is near the first AAA^+ domain of the motor unit (27, 51). As shown in Fig. 2B and C, a moderately strong ~150-kDa band (asterisk) and two faint bands at ~180 kDa and ~105 kDa were detected by the antibody 25-8 in the *oda2-t* axonemes, but none was detected by 12γB. In *oda2*, no band was detected by either antibody (a faint band at ~95 kDa is due to nonspecific binding). In the *oda2-t* pattern, the faint ~180-kDa band (arrow) could be the full-length product from the γ DHC gene of *oda2-t* (see below), and the ~150-kDa and ~105-kDa bands could have been generated by the proteolysis of the C-terminal sequence. The 150-kDa band is stronger than the 180-kDa band, possibly because the C-terminally attached NIT1 fragment (see below) assumes a disordered structure and is easily degraded. Polypeptides of 180 kDa and 150 kDa were also detected by Western blot analysis (Fig. 4C). These results indicate that *oda2-t* indeed expresses the N-terminal portion of the γ DHC, whereas *oda2* does not. Thus, it is likely that *oda2-t* axonemes contain a truncated form of the γ DHC.

The structure of the γ DHC gene in *oda2-t*. To examine the mutation in the γ *DHC* gene in detail, we first arbitrarily chose nine 500- to 1,500-bp sequences in the cDNA sequence (Fig. 3A) and examined whether the corresponding DNA fragments could be amplified by PCR from *oda2-t* genomic DNA. We found that the sequence corresponding to residues 3889 to 4363 of the registered cDNA sequence cannot be amplified but that the other eight fragments can be amplified. Since this observation suggested that *oda2-t* carries a gene insertion or deletion near the region that failed to amplify, we designed a 25-bp primer corresponding to residues 3381 to 3405 and carried out 3′ RACE with this and an abridged universal amplification primer using cDNA produced from the total *oda2-t* RNA. An ~2,000-bp DNA segment was obtained that contained partial sequences of the γ *DHC* and the *NIT1* genes. Double-strand cDNA was then amplified by PCR using primers designed based on the sequences of the γ *DHC* and the *NIT1* genes, followed by 3′ RACE. This resulted in the isolation of the cDNA corresponding to the γ *DHC* message expressed in this mutant. The amino acid sequence deduced from the cDNA sequence (Fig. 3B) indicated that the γ DHC in *oda2-t* has only 1,623 amino acids, containing a 1,270-amino-

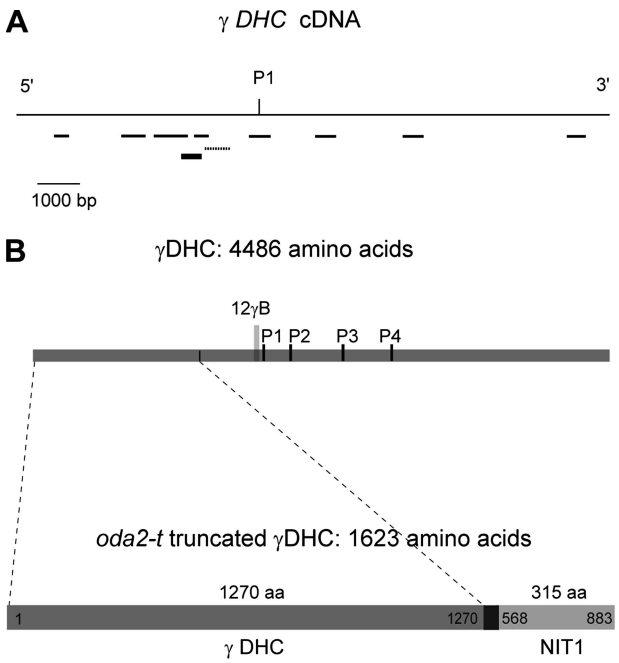

FIG. 3. Location of the *oda2-t* mutation within the γ *DHC* gene. (A) PCR amplification of *oda2-t* γ DHC genomic DNA fragments. DNA fragments that were amplified by PCR are shown by thin lines. The dotted line indicates the fragment that did not amplify. The thick line indicates the probe used for Southern blotting. P1 indicates the position of P-loop 1 (a phosphate-binding loop). (B) Domain organization of the truncated γ DHC in *oda2-t.* The N-terminal 1,270 amino acid residues of the γ DHC is joined with a 315-amino-acid sequence derived from the NIT1 gene, through a 38-amino-acid sequence (SAGARRRSFAPAWAVCTNPPFSPTAAPYPVTIVLSPTR) that is derived from a 94-bp vector sequence,18 bp of unknown origin, and 2 bp of the *NIT1* sequence.

acid sequence from the N-terminal region of the γ DHC and a 315-amino-acid sequence from the C-terminal region of the NIT1 protein connected by a 38-amino-acid adapter. The 114-base-pair sequence encoding the adapter contains 94 base pairs derived from the pUC119 vector sequence, 18 base pairs of unknown origin, and 2 base pairs from *NIT1*. The unidentified 18-bp sequence may be part of an intron of the γ *DHC* genomic sequence, which has not been determined previously. The molecular mass of the truncated γ DHC in *oda2-t* calculated from the determined sequence is 185,379 Da, including 146,931 Da of the N-terminal γ *DHC* sequence.

Subunit composition of the *oda2-t* outer-arm dynein. To examine the composition of the outer-arm dynein from *oda2-t*, we analyzed an axonemal high salt extract using ion-exchange chromatography with a Mono Q (9, 20) or a Uno Q column. The use of a Uno Q column allowed us to obtain a fraction that contains the full outer-arm complement of the α, β, and γ DHCs.

As shown in Fig. 4A, the elution pattern from the *oda2-t* extracts showed a significant reduction in the height of the peaks that would normally contain the γ DHC (fraction 2 [arrow]) and the α, β, and γ DHCs (fraction 19) but retained a peak that contains the α and β DHCs (fraction 24). SDS-PAGE and Western blotting showed that *oda2-t* axonemes lack the γ DHC but contain a novel polypeptide of an apparent molecular mass of 150 kDa (asterisk), corresponding to the N-terminal segment (for fractions 1 to 4 and 22 to 25) (Fig. 4C). In addition, an extra ~180-kDa band (arrow) is present for fractions 22 to 25. As for the Western blotting of the axonemes (Fig. 2), we interpret the ~180-kDa band to represent the full-length product and the ~150-kDa band to be a proteolytic fragment, the latter being predominant. We predict that fractions 1 to 4 correspond to a complex containing the truncated γ chain (including both the 150-kDa and 180-kDa polypeptides) and that fractions 22 to 25 correspond to a mixture of a complex containing the α, β, and truncated γ DHCs and a complex containing only the α and β DHCs.

Of the 11 LCs currently identified within the outer-arm dynein, LC1 (22 kDa) and LC4 (18 kDa) are known to associate with the γ DHC; LC1 is bound to the motor domain (2), and LC4 is permanently associated with the tail portion (26) and interacts in a Ca^{2+}-dependent manner with a region (residues 875 to 1182) containing two IQ motifs (44). As shown in Fig. 4B and C, in the wild-type axoneme, LC1 is present in the peak fraction of the γ DHC (fraction 2) and the αβγ DHCs (fraction 19), but it is totally absent in the corresponding fractions from *oda2-t* axonemes. In contrast, LC4 was found in both wild-type and *oda2-t* samples. Western blot patterns indicate that it is present in the fractions of the γ DHC (fraction 2) and the αβγ DHCs (fraction 19) of the wild type and in fractions 1 to 4 and 22 to 25 of *oda2-t*. Similarly, LC2 is present in both the wild type and *oda2-t*, in the fractions that contain the α and β DHCs but not in the fraction that contains only the γ DHC (fractions 1 to 4). These results and the SDS-PAGE patterns of the low-molecular-weight bands (Fig. 4B) are consistent with the previous report that LC1 and LC4 are, respectively, bound with the head and tail domains of the γ DHC, while other LCs are associated with the αβ DHCs or with the ICs. These observations also indicate that the truncated γ DHC remains stably associated with the αβ complex.

Electron microscope observations. In thin-section electron micrographs (Fig. 5A), *oda2-t* axonemes bear an average of 6.7 ± 1.5 (standard deviation) outer arms per nine outer doublets (n = 100). This is about 85% of the number in wild-type axonemes (7.9 ± 0.3, measured in samples prepared at the same time; Fig. 5B). Thus, *oda2-t* appears to have a slightly impaired ability to assemble outer dynein arms on the outer doublets. A similar reduction in the outer-arm number has been observed in *oda4-s7*, a mutant having outer arms with a truncated β DHC; in this case, the axoneme has been reported to have an average of 5.7 ± 1.1 outer arms (40).

When viewed in cross section, the outer arms in the *oda2-t* axonemes appeared somewhat thinner than those in the wild-type axonemes (Fig. 5A). To examine the difference in a more quantitative manner, we classified and averaged the individual outer-arm images using an image-clustering protocol. Two typical image groups of *oda2-t* axonemes are shown in Fig. 6A, together with the density difference from the averaged image of the wild-type outer arm. One group displays a major density difference in the inner lobe of the outer arm, while the other group shows two areas of density difference, one in the inner lobe, and the other in the outer side of the arm. In all groups of *oda2-t* outer-arm images, the density in the inner lobe (indicated by the green arrows in Fig. 6) was consistently found to be reduced, suggesting that the motor domain of the γ DHC is

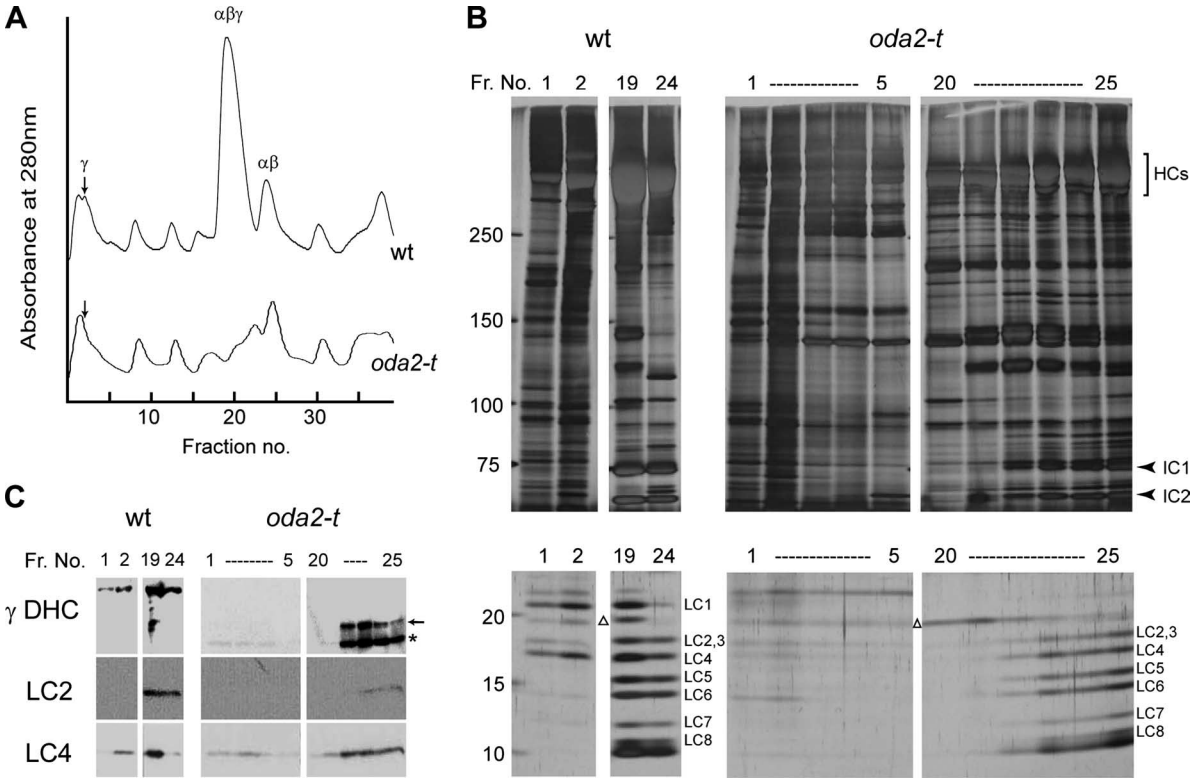

FIG. 4. Purification and composition of outer-arm dyneins from *oda2-t*. (A) The elution patterns of extracts from the wild-type and *oda2-t* axonemes. Axonemes were extracted with 0.6 M KCl, and the extracts were fractionated on a Uno Q column. Elution was carried out with a linear 80 to 300 mM KCl gradient. Note that the γ DHC peak (arrows) and the αβγ DHC peak are smaller for the *oda2-t* extracts than for those of the wild type. (B and C) SDS-PAGE patterns and Western blotting of the peak fractions (Fr.). (B) Heavy chains, intermediate-sized chains, and LCs were separated on a 5 to 20% gel (the central portion of the gel is not shown). LC1 is absent from the *oda2-t* lanes, whereas the other LCs, including LC4, are present. All gels were stained with silver. (C) Western blot analysis using antibody 25-8 (for the N-terminal region of γ DHC), R5391 (for LC2), and CT61 (for LC4). The 25-8 antibody detected the truncated γ DHC of *oda2-t* in fractions 1 to 4 and 22 to 25 (arrow and asterisk). The CT61 antibody detected LC4 in fractions where the γ DHC (in the wild type) and the truncated γ DHC (in *oda2-t*) are present. Western blotting using R5391 and the distribution pattern of the LCs indicates that the LC2 band overlaps with the LC3 band. A contaminating nondynein protein (indicated with a triangle) is present in the wild-type and *oda2-t* extracts above the LC2 band. These results are consistent with the SDS-PAGE analysis.

located in this region. It is interesting to note that in the cross-section images, the inner lobe of the outer arm appears to extend to the outer side of the inner-arm densities and that such an inner-lobe extension is still present in *oda2-t* (Fig. 6A). Figure 6B shows the typical averaged images of outer doublets in the axonemes of the wild type, *oda11*, *oda4-s7*, and *oda2-t*. As reported previously (39, 40), *oda11*, missing the α DHC, lacks density in the distal portion of the outer arm, and *oda4-s7*, in which the motor domain of the β DHC has been truncated, lacks density in a region between the inner lobe and the tip.

Motility. The swimming velocity and flagellar beat frequency in *oda2-t*, *oda2*, *oda4-s7*, *oda11*, and the wild type are compared in Fig. 7. The swimming velocity of *oda2-t* is much lower than that of the wild type, but interestingly, it is significantly higher than that of *oda2*, a mutant lacking outer arms (Fig. 7A). A comparison of these five strains revealed that their average swimming velocities are in the following order, from highest to lowest: the wild type, *oda11*, *oda2-t*, and *oda4-s7* and *oda2*, which were approximately equal (Fig. 7B). The same order was observed for the flagellar beat frequency, as determined from the power spectra of swimming cells (Fig. 7C). The spectrum of *oda2-t* has a peak at about 50 Hz, while the spectra of *oda4-s7* and *oda2* have peaks at about 30 Hz. These results suggest that outer-arm dyneins lacking γ DHC motor domains can function to some extent, while outer arms missing β DHC motor domains are almost completely nonfunctional.

Chlamydomonas flagella display Ca^{2+}-dependent waveform conversion, such that the axonemes beat in an asymmetrical, ciliary pattern at Ca^{2+} concentrations lower than 10^{-6} M while they beat in a symmetrical flagellar pattern at Ca^{2+} concentrations higher than 10^{-5} M (3, 16). The conversion to the flagellar pattern is observed in live cells when displaying transient backward swimming upon illumination with intense light. Outer-arm dyneins are important for waveform conversion, as *oda* mutants lacking outer arms do not display this light-induced backward swimming (24). The Ca^{2+}-binding LC4 has been suggested to have a role in this waveform conversion (26, 42). To determine whether the outer-arm dynein of *oda2-t*, which retains LC4 as well as the α and β DHCs, can effectively function in waveform conversion, the motility of the *oda2-t* axonemes at 10^{-4} M Ca^{2+} was examined. When motility was reactivated by the addition of ATP at 10^{-8} M Ca^{2+}, >80% of the wild-type axonemes and ~50% of the *oda2* and *oda2-t*

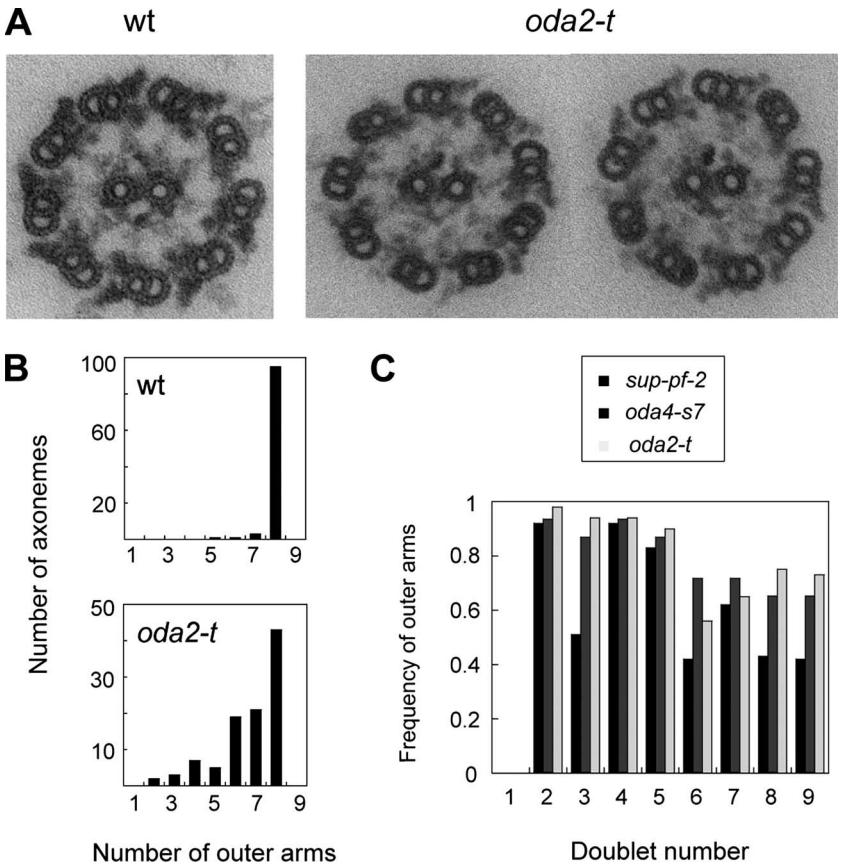

FIG. 5. Electron microscopic analysis of the *oda2-t* axonemes. (A) Wild-type (wt) and *oda2-t* cross sections. Note that the outer-arm images for *oda2-t* appear thinner than for the wild type and are frequently missing or are weakened on some outer-doublets. (B) Number of the outer-doublet microtubules that bear outer arms in axonemal cross sections. (C) The average frequency of the presence of outer arms on particular outer doublets. The number of images used was 43 for *oda2-t* and 32 for *oda4-s7*. The data for *sup-pf-2* are from Rupp et al. (38). In the wild-type axonemes, the outer doublet that lacks outer-arm dyneins is doublet no. 1, and other outer doublets are numbered clockwise in cross sections viewed from the base to tip direction (as in Fig. 5A). In the proximal region of the axoneme, the B tubule of doublets 1, 5, and 6 have beak-like structures (13), which serve as markers for numbering. These beaks are clearly seen in the two *oda2-t* images in panel A. In 25 wild-type images, the average numbers of outer arms were 0.0 for doublet 1 and 1.0 for all other doublets.

axonemes in solution displayed beating with similar asymmetrical waveforms (Fig. 7D). At 10^{-4} M Ca^{2+}, ~60% of the wild-type axonemes were motile and all displayed beating with a symmetrical waveform moving straight in the medium at a velocity of 140.2 ± 29.3 μm/s (average ± standard deviation for 20 moving axonemes). In contrast, only <10% of the *oda2* axonemes beat and did so with a symmetrical waveform of very small amplitude (Fig. 7D). These data are consistent with the observations of Mitchell and Rosenbaum (29). The beating of *oda2* axonemes was so ineffective that it did not result in the efficient propulsion of the axoneme; the velocity of movement was only 3.5 ± 1.3 μm/s (n = 20), i.e., about 1/40 of the wild-type speed. The movement of the *oda2-t* axonemes at 10^{-4} M Ca^{2+} was much the same as that of *oda2*; the axonemes moved at 5.74 ± 1.4 μm/s (n = 20). These results suggest that outer-arm dyneins without the γ DHC motor unit cannot contribute to the generation of symmetrical waveforms that cause effective propulsive force, even though LC4 is retained.

ATPase activities. The ATPase activities of the wild-type and mutant axonemes, either before or after extraction with 0.6 M KCl, are compared in Table 1. The values are expressed as the amount of phosphate liberated per unit time by a constant amount of axonemes. We used solution conditions in which axonemes displayed beating for longer than 10 min and checked that the phosphate liberation was linear with time for at least the initial 5 min. The axonemal ATPase activities thus measured were several times higher than those reported previously but consistent with the values obtained by Yagi and Kamiya (53) who used similar solution conditions. As reported previously (8, 19), the ATPase activity of axonemes is significantly higher than the sum of the activities in the high-salt extract and the extracted axonemes, indicating that the dynein ATPase is activated in situ. This activation is most likely caused by the interaction of dynein with the doublet microtubules.

Several features of the axonemal ATPase activities are noteworthy. First, as previously reported, ATPase activity was very low in axonemes that lack the entire outer arm (14, 19, 29). More than 75% of the ATPase activity in wild-type axonemes can be accounted for by the activity of outer-arm dyneins. Second, the ATPase activity in *oda4-s7* was markedly lower than the activities of other mutant axonemes with partial

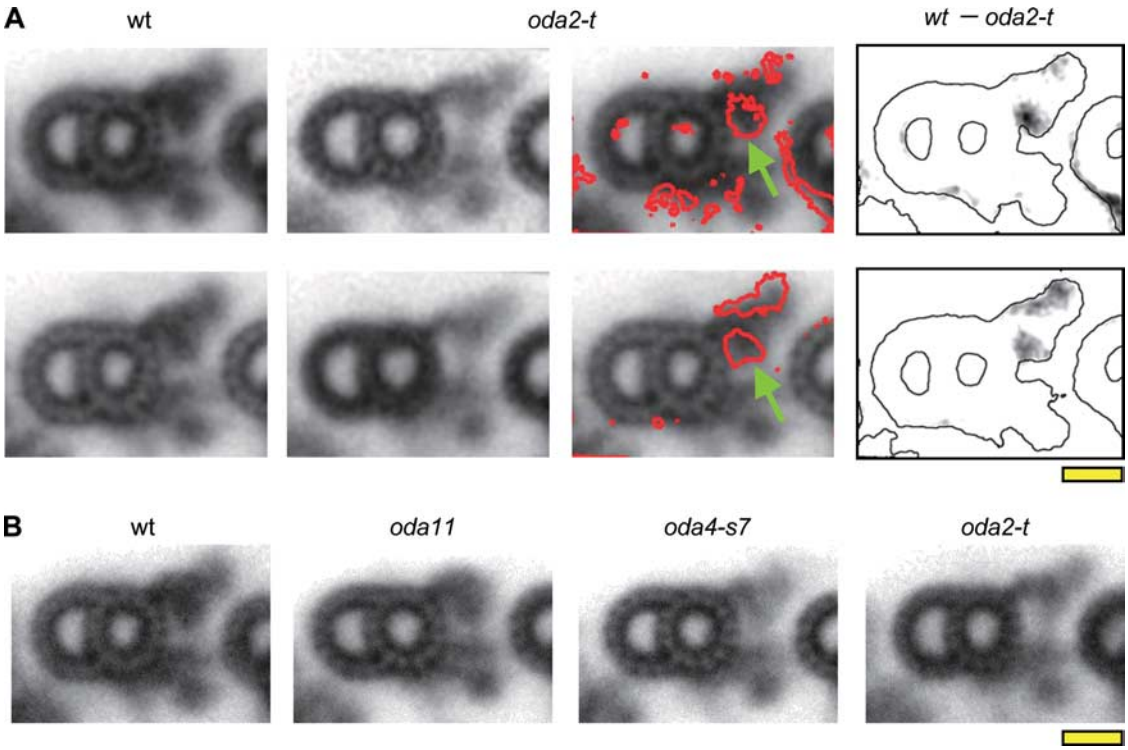

FIG. 6. Averaged images of outer doublet cross sections. (A) The statistical difference between outer-arm dyneins from *oda2-t* and the wild type. Two typical wild-type images (first column) and two typical images of *oda2-t* (second column) obtained by cluster analysis are shown. The red contours on the wild-type images (third column) show the differences between the wild type and *oda2-t* at a 99% confidence level determined by the Student *t* test. The difference in density between the wild type and *oda2-t* (fourth column) are superimposed onto the outlines of the wild-type images. The motor domain of the γ DHC is most likely located in the proximal region of the outer arm indicated by the green arrows. (B) Averaged outer-arm images from the wild-type (wt), *oda11*, *oda4-s7*, and *oda2-t* axonemes. The averaged images of the largest cluster are shown. The number of images used was 22 (wild type), 23 (*oda11*), 17 (*oda4-s7*), and 22 (*oda2-t*). Bar, 10 nm.

outer-arm defects, indicating the importance of the β DHC for the high ATPase activity in the axoneme. Finally, and most strikingly, the ATPase activity of the *oda2-t* axonemes was higher than those of the wild type.

Lack of a suppressor activity. Previously, a *sup-pf-2* mutant was isolated that has an activity that suppresses the paralyzed-flagella phenotype of mutants deficient in the central pair microtubules or radial spokes (15). It was later shown to have a mutation in the γ *DHC* gene (38), and a number of additional alleles have been isolated (28, 38). An interesting feature in one of the *sup-pf-2* alleles is that the number of outer arms in the axonemal cross section is reduced and the degree of the reduction is biased toward a subset of outer-doublet microtubules; outer arms are more often missing on doublets 3 and 6 to 9 than on other doublets (38; for doublet numbering, see the legend to Fig. 5 and reference 13). However, since the defects in the γ *DHC* genes of other *sup-pf-2* alleles have not been determined, it is not understood whether the suppressor activity results from a specific class of γ *DHC* mutations or from a general loss of its motile activity in the background of unimpaired α and β DHCs. Nor is the relationship between the suppressor activity and the position of the outer-arm loss known.

To answer these questions, we examined whether *oda2-t* exhibits suppressor activity and counted the number of outer arms on specific outer doublets. We found that double mutants between *oda2-t* and *pf14*, lacking the radial spokes, and between *oda2-t* and *pf18*, missing the central pair, did not show flagellar beating. Therefore, *oda2-t* does not have a suppressor activity. On the other hand, the loss of outer arms in *oda2-t* was found to be biased among the outer doublets, such that doublets 6 to 9 tended to show greater loss than doublets 2 to 5 (doublet number 1 lacks outer arms even in the wild-type axonemes; 13) (Fig. 5C). Interestingly, a similar bias was also observed with the *oda4-s7* β *DHC* mutant. Therefore, doublets 6 to 9 may have a general tendency to lose outer arms more frequently than doublets 2 to 5 when the outer arm has an unstable structure. This bias could be a consequence of the beat pattern of *Chlamydomonas* flagella, which must produce asymmetric distortion within the axoneme.

DISCUSSION

In this study we isolated a novel *Chlamydomonas* mutant, the *oda2-t* strain, which expresses a truncated γ DHC consisting of the N-terminal third of the molecule. This mutant retains outer dynein arms containing the α and β DHCs, whereas the previously isolated *oda2* γ *DHC* mutant lacks the entire outer arm. This difference in phenotype clearly indicates that the N-terminal portion of the γ DHC, corresponding to the tail, is important for the assembly of the outer arm on the outer doublet microtubules. The *oda2-t* mutant is reminiscent of the

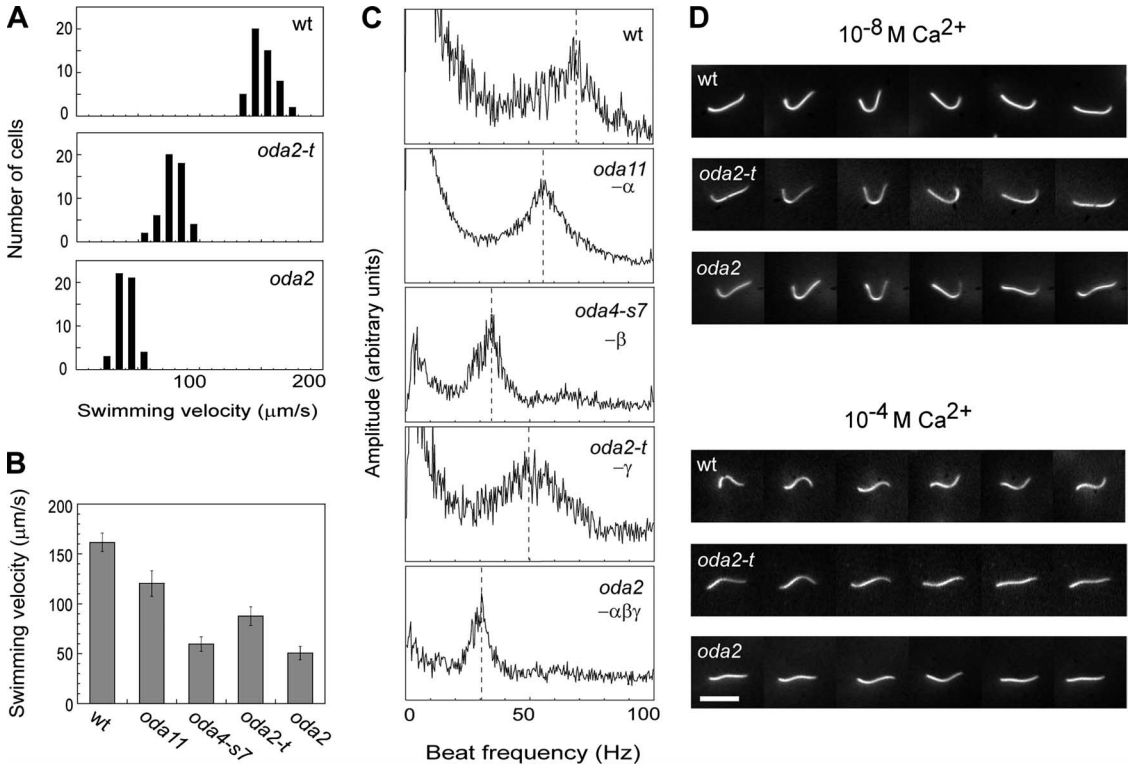

FIG. 7. Motility analysis. (A) Swimming velocities of wild-type, *oda2-t*, and *oda2* live cells ($n = 50$). The average velocity (standard deviation) for each strain (μm/s) was as follows: the wild type, 161.6 (9.2); *oda2-t*, 87.8 (9.4); and *oda2*, 50.6 (6.6). (B) Comparison of the average swimming velocities for the wild type and mutants deficient in outer-arm DHCs ($n = 50$). (C) Flagellar beat frequencies for the wild type and mutants deficient in outer-arm DHCs measured using the FFT method (22). (D) Images of isolated axonemes beating in a medium containing 1 mM ATP and 10^{-8} M or 10^{-4} M Ca^{2+}. Six images are shown for a single axoneme with variable time intervals so as to illustrate the sequence of beat pattern. The beat frequency (standard deviation) measured for 20 axonemes under these conditions was as follows: at 10^{-8} M Ca^{2+}, 69.5 (11.4) Hz for the wt, 48.4 (3.4) Hz for *oda2-t*, and 28.8 (2.8) Hz for *oda2*, and at 10^{-4} M Ca^{2+}, 78.7 (13.2) Hz for the wt, 14.5 (2.7) Hz for *oda2-t*, and 15.1 (4.8) Hz for *oda2*. Temperature, 25°C. Bar, 10 μm.

oda4-s7 mutant, which expresses a truncated β DHC of approximately one-third the normal size; it retains outer arms containing the α and γ DHCs, in contrast with the previously isolated *oda4* mutant, which lacks the entire outer arm (40). Unlike these DHCs, the α DHC is dispensable for outer-arm assembly; *oda11*, which lacks this DHC, assembles outer arms that contain the β and γ DHCs (39). Consistent with this observation, the N-terminal sequence of the α DHC differs significantly from that of the β or γ DHC (30, 51; T. Yagi, unpublished results).

Electron microscopic observations of axonemal cross sections, in combination with cluster analysis, have clearly shown that the outer-arm images in *oda2-t* lack the electron density at the innermost lobe located near the A tubule. Some classes of images showed, in addition to the change in the innermost lobe, a wedge-shaped area of density change on the outer side of the entire outer arm. However, this latter difference could be explained by an alteration in the orientation of the entire arm, which might well be caused by the loss of the proximal structure. Thus, all observations are consistent with the γ DHC motor unit being located at the innermost lobe of the outer arm. This localization is as predicted from previous studies on mutants lacking the α and β DHCs (39, 40). Recent studies using cryoelectron tomography (17, 33) or three-dimensional reconstruction from cryoelectron microscopic images (34) have indicated that the motor domains of the three outer-arm DHCs are stacked against each other, such that the three AAA^+ rings are aligned at a shallow angle to the wall of the A tubule. A striking feature is that the motor domain of the most proximal DHC, which is the γ DHC as judged from the images of the mutants, is located very close to the microtubule wall, almost attaching to it. Therefore, the presence of the γ DHC may be critically important for the attachment of the entire outer arm to the microtubule at a fixed angle.

The swimming velocity and flagellar beat frequency of *oda2-t*

TABLE 1. Axonemal ATPase activity in the wild type and mutants deficient in outer-arm DHCs[a]

Strain	Missing DHC	Axonemes	High-salt extract	Extracted axonemes
Wild type		1.59 (0.08)	0.41 (0.02)	0.12 (0.039)
oda11	α	1.30 (0.10)	0.67 (0.004)	0.054 (0.013)
oda4-s7	β	0.60 (0.06)	0.08 (0.02)	0.054 (0.006)
oda2-t	γ	2.03 (0.30)	0.27 (0.02)	0.052 (0.002)
oda2	αβγ	0.35 (0.04)	0.01 (0.001)	0.039 (0.010)

[a] Values are the averages and standard deviations (in parentheses) of the results from three independent samples, given in units of μmol phosphate released/minute/mg axonemes.

were much lower than those of the wild type and *oda11* but significantly higher than those of *oda2* and *oda4-s7*. In view of the finding that the loss of the γ DHC motor domain produces a large change in the alignment of the outer arms, it is somewhat surprising that this deficiency does not completely impair outer-arm function, whereas the lack of the β DHC motor unit in *oda4-s7* results in a total loss of motor activity. Thus, from a phenomenological point of view, the β DHC is the most important power generator among the three DHCs of the outer arm. Studies that compared outer-arm structure in the presence and absence of ATP/vanadate demonstrated that the outer arm undergoes a large structural change during the mechanochemical cycle (34, 49). In terms of the change in relative position upon nucleotide binding, the α DHC displays the largest change, the β DHC an intermediate change, and the γ DHC almost no change (34). The observed large positional alteration in structure may result from the concerted action of the three DHCs and the γ DHC positioned at the base may exert the greatest influence on the overall structure of the outer arm (see Fig. 6A). However, the present findings indicate that the outer arm can function to some extent even without the γ DHC.

Despite the presence of partially functional outer-arm dyneins with truncated γ DHCs that retain the calcium-binding LC4, *oda2-t* axonemes, unlike wild-type axonemes, did not display effective beating with symmetrical waveforms at 10^{-4} M Ca^{2+}. This finding suggests that the γ DHC is important for axonemal beating at high Ca^{2+} concentrations. Since LC4 has been suggested to play a role in the Ca^{2+}-dependent waveform conversion (44), this further suggests that there is a tight functional interaction between LC4 and the motor domain of the γ DHC. In other words, LC4 possibly controls waveforms through the DHC to which it binds.

Comparison of the ATPase activities in outer-arm-deficient axonemes revealed several interesting features. Most notably, the axonemes of *oda2-t* have higher ATPase activity than those of the wild type. This result suggests that in the wild-type outer-arm dynein, the γ DHC is somehow inhibiting the microtubule-activated ATPase activity of the α and β DHCs. Previously, Nakamura et al. (32) examined the ATPase activities of an 18S subparticle of the outer-arm dynein containing the α and β DHCs and a 12S subparticle containing the γ DHC and showed that the γ DHC suppressed the ATPase activity of the αβ DHC subparticle when the subparticles reassociate. Our present finding is in good agreement with their conclusion. Another interesting feature is that the ATPase activity of *oda11* axonemes is close to that of the wild type, and the activity in the *oda11* high-salt extract is even higher than that in the wild-type extract. Our observations are consistent with the previous report that the α DHC suppresses the ATPase activity of the β DHC in purified samples (37) and apparently controls ATP-dependent microtubule binding by the β and γ DHCs (42). Taken together, the ATPase activity of the outer-arm dynein, with or without activation by microtubules, must be regulated through the interactions between the different DHCs or their associated components. The observation that the *oda11* and *oda2-t* axonemes have high ATPase activities yet display much poorer motility than those of the wild type suggests that these axonemes have defects in mechanochemical coupling, which is likely to be regulated through interactions between DHCs as well as between dyneins and microtubules.

For an understanding of how an outer-arm dynein functions, we need to understand the properties of individual DHCs as motor proteins, as well as their structures and the manner of assembly of the arm. The use of *Chlamydomonas* mutants has been the most powerful approach to this end. However, recently, motility analysis using *Trypanosoma* in combination with gene knockdown by RNA interference has started to provide novel insights (1, 5). For example, the outer-arm dynein of this organism has been shown to play a key role in the switching of the beat propagation direction (1, 5). Combined studies using *Chlamydomonas* forward genetics and *Trypanosoma* reverse genetics will yield further important information as to how outer arms function, and the data obtained from these organisms will complement each other. The availability of *Chlamydomonas* mutants lacking the motor domain of any one of the three outer-arm DHCs implies that the use of appropriate biochemical techniques and single and double mutants will enable us to obtain outer-arm dyneins with any desired combination of motor domains. These altered dyneins will greatly facilitate studies aimed at understanding how the outer arm functions.

ACKNOWLEDGMENTS

We thank Gianni Piperno (Mt. Sinai Hospital) for kindly providing monoclonal antibody 25-8, Masafumi Hirono (University of Tokyo) for advice on gene analysis, Susumu Aoyama (University of Tokyo) for help with video-microscopy, and Akane Furuta (University of Tokyo) for help with ATPase measurements.

This study has been supported by grants-in-aid from the Ministry of Education, Culture, Sports, Science and Technology of Japan to R.K. and by grant GM51293 from the National Institutes of Health to S.M.K.

REFERENCES

1. **Baron, D. M., Z. P. Kabututu, and K. L. Hill.** 2007. Stuck in reverse: loss of LC1 in *Trypanosoma brucei* disrupts outer dynein arms and leads to reverse flagellar beat and backward movement. J. Cell Sci. **120:**1513–1520.
2. **Benashski, E. S., S. R. Patel-King, and S. M. King.** 1999. Light chain 1 from the *Chlamydomonas* outer dynein arm is a leucine-rich repeat protein associated with the motor domain of the γ heavy chain. Biochemistry **38:**7253–7264.
3. **Bessen, M., R. B. Fay, and G. B. Witman.** 1980. Calcium control of waveform in isolated flagellar axonemes of *Chlamydomonas*. J. Cell Biol. **86:**446–455.
4. **Blum, H., H. Beier, and H. J. Gross.** 1987. Improved silver staining of plant proteins, RNA and DNA in polyacrylamide gels. Electrophoresis **8:**93–99.
5. **Branche, C., L. Kohol, G. Toutirais, J. Buisson, J. Cosson, and P. Bastin.** 2006. Conserved and specific functions of axoneme components in *Trypanosome* motility. J. Cell Sci. **15:**3443–3455.
6. **DiBella, L. M., O. Gorbatyuk, M. Sakato, K. Wakabayashi, R. S. Patel-King, G. J. Pazour, G. B. Witman, and S. M. King.** 2005. Differential light chain assembly influences outer arm dynein motor function. Mol. Biol. Cell **16:**5661–5674.
7. **Frohman, M. A., M. K. Dush, and G. R. Martin.** 1988. Rapid production of full-length cDNAs from rare transcripts: amplification using a single gene-specific oligonucleotide primer. Proc. Natl. Acad. Sci. USA **85:**8998–9002.
8. **Gibbons, I. R., and E. Fronk.** 1979. A latent adenosine triphosphatase form of dynein 1 from sea urchin sperm flagella. J. Biol. Chem. **254:**187–196.
9. **Goodenough, U. W., B. Gebhart, V. Mermall, D. R. Mitchell, and J. E. Heuser.** 1987. High-pressure liquid chromatography fractionation of *Chlamydomonas* dynein extracts and characterization of inner-arm dynein subunits. J. Mol. Biol. **194:**481–494.
10. **Goodenough, U. W., and J. E. Heuser.** 1982. Substructure of the outer dynein arm. J. Cell Biol. **95:**798–815.
11. **Goodenough, U. W., and J. E. Heuser.** 1984. Structural comparison of purified dynein proteins with *in situ* dynein arms. J. Mol. Biol. **180:**1083–1118.
12. **Harris, E.** 1989. The *Chlamydomonas* sourcebook. Academic Press, San Diego, CA.
13. **Hoops, H. J., and G. B. Witman.** 1983. Outer doublet heterogeneity reveals

structural polarity related to beat direction in *Chlamydomonas* flagella. J. Cell Biol. **97:**902–908.
14. **Huang, B., G. Piperno, and D. J. L. Luck.** 1979. Paralyzed flagella mutants of *Chlamydomonas reinhardtii* defective for axonemal doublet microtubule arms. J. Biol. Chem. **254:**3091–3099.
15. **Huang, B., Z. Ramanis, and D. J. Luck.** 1982. Suppressor mutations in *Chlamydomonas* reveal a regulatory mechanism for flagellar function. Cell **28:**115–124.
16. **Hyams, J. S., and G. G. Borisy.** 1978. Isolated flagellar apparatus of *Chlamydomonas*: characterization of forward swimming and alteration of waveform and reversal of motion by calcium ions in vitro. J. Cell Sci. **33:**235–253.
17. **Ishikawa, T., H. Sakakibara, and K. Oiwa.** 2007. The architecture of outer dynein arms *in situ*. J. Mol. Biol. **368:**1249–1258.
18. **Johnson, K. A., and J. S. Wall.** 1983. Structure and molecular weight of the dynein ATPase. J. Cell Biol. **96:**669–678.
19. **Kagami, O., and R. Kamiya.** 1990. Strikingly low ATPase activities in flagellar axonemes of a *Chlamydomonas* mutant missing outer dynein arms. Eur. J. Biochem. **189:**441–446.
20. **Kagami, O., and R. Kamiya.** 1992. Translocation and rotation of microtubules caused by multiple species of *Chlamydomonas* inner-arm dynein. J. Cell Sci. **103:**653–664.
21. **Kamiya, R.** 1988. Mutations at twelve independent loci result in absence of outer dynein arms in *Chlamydomonas reinhardtii*. J. Cell Biol. **107:**2253–2258.
22. **Kamiya, R.** 2000. Analysis of cell vibration for assessing axonemal motility in *Chlamydomonas*. Methods **22:**383–387.
23. **Kamiya, R.** 2002. Functional diversity of axonemal dynein as studied in *Chlamydomonas* mutants. Int. Rev. Cytol. **219:**115–155.
24. **Kamiya, R., and M. Okamoto.** 1985. A mutant of *Chlamydomonas reinhardtii* that lacks the flagella outer arm but can swim. J. Cell Sci. **74:**181–191.
25. **King, S. M., and R. Kamiya.** Axonemal dyneins: assembly, structure and force generation. *In* G. B. Witman (ed.), *Chlamydomonas* source book, vol. III, in press. Elsevier Press, Amsterdam, The Netherlands.
26. **King, S. M., and R. S. Patel-King.** 1995. Identification of a Ca^{2+}-binding light chain within *Chlamydomonas* outer arm dynein. J. Cell Sci. **108:**3757–3764.
27. **King, S. M., and G. B. Witman.** 1988. Structure of the γ heavy chain of the outer arm dynein from *Chlamydomonas* flagella. J. Cell Biol. **107:**1799–1808.
28. **Mitchell, B. F., L. E. Grulich, and M. M. Mader.** 2004. Flagellar quiescence in *Chlamydomonas*: characterization and defective quiescence in cells carrying *sup-pf-1* and *sup-pf-2* outer dynein arm mutations. Cell Motil. Cytoskelet. **57:**186–196.
29. **Mitchell, D. R., and J. L. Rosenbaum.** 1985. A motile *Chlamydomonas* flagella mutant that lacks outer dynein arms. J. Cell Biol. **100:**1228–1234.
30. **Mitchell, D. R., and K. S. Brown.** 1997. Sequence analysis of the *Chlamydomonas reinhardtii* flagellar α dynein gene. Cell Motil. Cytoskelet. **37:**120–126.
31. **Moss, A. G., W. S. Sale, L. A. Fox, and G. B. Witman.** 1992. The α subunit of sea urchin outer arm dynein mediates structural and rigor binding to microtubules. J. Cell Biol. **87:**1189–1200.
32. **Nakamura, K., C. G. Wikerson, and G. B. Witman.** 1997. Functional interaction between *Chlamydomonas* outer arm dynein subunits: the γ subunit suppresses the ATPase activity of the αβ dimer. Cell Motil. Cytoskelet. **37:**338–345.
33. **Nicastro, D., C. Schwartz, J. Pierson, R. Gaudette, M. E. Porter, and J. R. McIntosh.** 2006. The molecular architecture of axonemes revealed by cryoelectron tomography. Science **313:**944–948.
34. **Oda, T., N. Hirokawa, and M. Kikkawa.** 2007. Three-dimensional structures of the flagellar dynein-microtubule complex by cryoelectron microscopy. J. Cell Biol. **177:**243–252.
35. **Patel-King, R. S., S. E. Benashski, A. Harrison, and S. M. King.** 1997. A *Chlamydomonas* homologue of the putative murine *t* complex distorter Tctex-2 is an outer arm dynein light chain. J. Cell Biol. **137:**1081–1090.
36. **Perrone, C. A., S. H. Myster, R. Bower, E. T. O'Toole, and M. E. Porter.** 2000. Insights into the structural organization of the I1 inner arm dynein from a domain analysis of the 1β dynein heavy chain. Mol. Biol. Cell **11:**2297–2313.
37. **Pfister, K. K., and G. B. Witman.** 1984. Subfractionation of *Chlamydomonas* 18 S dynein into two unique subunits containing ATPase activity. J. Biol. Chem. **259:**12072–12080.
38. **Rupp, G., E. O'Toole, L. C. Gardner, B. F. Mitchell, and M. E. Porter.** 1996. The *sup-pf-2* mutations of *Chlamydomonas* alter the activity of the outer dynein arms by modification of the γ-dynein heavy chain. J. Cell Biol. **135:**1853–1865.
39. **Sakakibara, H., D. R. Mitchell, and R. Kamiya.** 1991. A *Chlamydomonas* outer arm dynein mutant missing the α heavy chain. J. Cell Biol. **113:**615–622.
40. **Sakakibara, H., S. Takada, S. M. King, G. B. Witman, and R. Kamiya.** 1993. A *Chlamydomonas* outer arm dynein mutant with a truncated β heavy chain. J. Cell Biol. **122:**653–661.
41. **Sakakibara, H., and H. Nakayama.** 1998. Translocation of microtubules caused by the αβ, β and γ outer arm dynein subparticles of *Chlamydomonas*. J. Cell Sci. **111:**1155–1164.
42. **Sakato, M., and S. M. King.** 2003. Calcium regulates ATP-sensitive microtubule binding by *Chlamydomonas* outer arm dynein. J. Biol. Chem. **278:**43571–43579.
43. **Sakato, M., and S. M. King.** 2004. Design and regulation of the AAA^{+} microtubule motor dynein. J. Struct. Biol. **146:**58–71.
44. **Sakato, M., H. Sakakibara, and S. M. King.** 2007. *Chlamydomonas* outer arm dynein alters conformation in response to Ca^{2+}. Mol. Biol. Cell **18:**3620–3634.
45. **Sale, W. S., and L. Fox.** 1988. Isolated β heavy chain subunit of dynein translocates microtubules in vitro. J. Cell Biol. **107:**1793–1797.
46. **Smith, E. F., and P. A. Lefebvre.** 1996. PF16 encodes a protein with armadillo repeats and localizes to a single microtubule of the central apparatus in *Chlamydomonas* flagella. J. Cell Biol. **132:**359–370.
47. **Takada, S., H. Sakakibara, and R. Kamiya.** 1992. Three-head outer arm dynein from *Chlamydomonas* that can functionally combine with outer-arm-missing axonemes. J. Biochem. **111:**758–762.
48. **Tam, L. W., and P. A. Lefebvre.** 1993. Cloning of flagellar genes in *Chlamydomonas reinhardtii* by DNA insertional mutagenesis. Genetics **135:**375–384.
49. **Tsukita, S., S. Tsukita, J. Usukura, and H. Ishikawa.** 1983. ATP-dependent structural changes of the outer dynein arm in *Tetrahymena* cilia: a freeze-etch replica study. J. Cell Biol. **96:**1480–1485.
50. **Weeks, D. P., N. Beerman, and O. M. Griffith.** 1986. A small-scale five-hour procedure for isolating multiple samples of CsCl-purified DNA: application to isolations from mammalian, insect, higher plant, algal, yeast, and bacterial sources. Anal. Biochem. **152:**376–385.
51. **Wilkerson, C. G., S. M. King, and G. B. Witman.** 1994. Molecular analysis of the γ heavy chain of *Chlamydomonas* flagella outer-arm dynein. J. Cell Sci. **107:**497–506.
52. **Witman, G. B., K. A. Johnson, K. K. Pfister, and J. S. Wall.** 1983. Fine structure and molecular weight of the outer arm dyneins of *Chlamydomonas*. J. Submicrosc. Cytol. **15:**193–197.
53. **Yagi, T., and R. Kamiya.** 2000. Vigorous beating of *Chlamydomonas* axonemes lacking central pair/radial spoke structures in the presence of salts and organic compounds. Cell Motil. Cytoskelet. **46:**190–199.
54. **Yagi, T., I. Minoura, A. Fujiwara, R. Saito, T. Yasunaga, M. Hirono, and R. Kamiya.** 2005. An axonemal dynein particularly important for flagellar movement at high viscosity: implications from a new *Chlamydomonas* mutant deficient in the dynein heavy chain gene *Dhc9*. J. Biol. Chem. **280:**41412–41420.
55. **Yasunaga, T., and T. Wakabayashi.** 1996. Extensible and object-oriented system Eos supplies a new environment for image analysis of electron micrographs of macromolecules. J. Struct. Biol. **116:**155–160.